

INSIGHTS IN TO MILNACIPRAN INTERACTIONS WITH BOVINE SERUM ALBUMIN

Lade Somaji^{1*}, Ravi Rapolu²

¹Research Scholar, Mewar University, Chittorgarh, Rajasthan, India

²Research Supervisor, Mewar University, Chittorgarh, Rajasthan, India.

Email : somunichem@gmail.com

Abstract:

Milnacipran HCl (MCP), an antidepressant drug used for treating depression belongs to serotonin and norepinephrine reuptake inhibitor class of compounds. High bioavailability of MCP besides its rapid absorption and elimination makes it a selective drug for prescription. On the other hand, MCP has poor affinity towards transporting proteins. To date, there are no detailed studies which accounts for the poor affinity of MCP with transporting proteins. Herein the present study brings out the binding capacity of MCP with model transporting protein BSA by spectroscopic and molecular modelling studies. Fluorescence studies demonstrated that MCP interacts with BSA with a binding constant of $5.32 \pm 1.5 \times 10^4 \text{M}^{-1}$ by forming complex (static quenching) besides collisions (dynamic quenching). During interaction with MCP, 6% of helical content of BSA was reduced and formed complex is stable up to 75°C as evident from CD studies. MCP interacts with BSA at junction of domain I and domain II by forming hydrogen bonds with TYR 89 and ASP 86 and the aromatic ring of MCP involves in the hydrophobic interactions (Pi-Pi and Pi-Sulphur).

Keywords —Milnacipran, Antidepressants, serotonin, and norepinephrine reuptake inhibitors (SNRIs), Bovine Serum Albumin.

I. INTRODUCTION

Human emotional outcomes (behaviors) are the aftermath of individual's social, psychological, and biological ingredients that results in short to long-lived responses. Short-lived responses are merely due to usual fluctuations in the mood and are of not much concerned. However, long-lived responses to the life events such as unemployment, stress, and bereavement to name a few may lead to the complex illness termed as depression. This situation of depression engenders an imbalance in the neurotransmitter's concentrations in the synaptic cleft thereby leading to the psychiatric behavior. To restore balance of these neurotransmitters' antidepressants were deployed. Among the antidepressants that were deployed, milnacipran (MCP) belongs to serotonin and norepinephrine

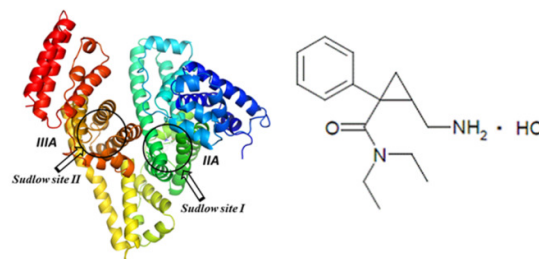
reuptake inhibitors (SNRIs) class of compounds and offers several advantages over other tricyclic depressants and selective serotonin reuptake inhibitors (SSRIs). Notable advantages of milnacipran are high bioavailability, rapid absorption and elimination, minimal drug interactions which makes it a choice of drug for treating depression. Besides these pharmacodynamic and pharmacokinetic properties it has poor affinity towards proteins and particularly towards CYP450 enzymes, thereby limiting the metabolism of MCP. Further MCP binds only up to 13% of administered drug dosage towards serum albumins implying that albumins might have minimal role in transporting MCP.

On the other hand, serum albumins are known to be the major circulating plasma proteins which

bound various chemical entities (drugs, exogenous and endogenous molecules) with high binding capacities and regulates their distribution in the body fluids[1]. Albumins are also known to act as reservoirs for nitric oxide which entails key role in various physiological process, including neurotransmission[2]. Not limiting to these, albumins are known to be the key pharmacological modulators of the most of drugs by controlling their active and free concentrations in the body, consequently determining the drug action and its effects. Hence, it is imperative to understand the functional role of albumin in transporting MCP to the site of action.

In the present study, we aimed to unravel the interaction mechanism of MCP with plasma proteins by taking bovine serum albumin (BSA) as a model protein. Besides its structural homology of $\approx 76\%$ with human serum albumin, it is medically important, stable, versatile ligand binding properties and low cost made it choice of protein for the present study[3,4]. BSA is single polypeptide chain having 582 amino acid residues and is subdivided into three homologues domains I, II and III which are further divided into subdomains A and B[5]. These domains are interlinked by 17 cystine residues among which 16 cystine residues are involved in formation of eight disulfide bonds and one cystine residue remains free. BSA contains two tryptophan's (W134 and W213) located each in domain I and II respectively. As the present study brings out the bioavailability of MCP in terms of its binding constant, pharmacological modulation of MCP can be achieved thereby influencing the transport activity. This modulation further act upon variety of neurophysiological process and can be utilized in the treatment of psychiatric disease. The 3D pictorial representation structure of BSA and chemical structure of MCP is given in Figure 1.

Fig. 1 3D pictorial structure of Bovine serum albumin (BSA) and chemical structure of Milnacipran HCL (MCP)



II. MATERIAL AND METHODS

Materials

Milnacipran HCL (MCP) is procured as a gift sample from laurel pharma Labs, Hyderabad, India. Bovine Serum albumin (BSA) is purchased from Himedia. Stock Solution of 1mM MCP is prepared in methanol and further diluted with 100mM Tris-HCl (pH=7.4) to achieve a final working stock concentration of 0.1mM. 1mM stock solutions of site markers, phenylbutazone (PBZ) and ibuprofen (IBU) are prepared in DMSO and further diluted with 100mM Tris-HCl to achieve a working stock solution of 0.1mM. All solvents used in the present study were of analytical grade.

Methods

0.5 μ M of BSA is used as working solution for performing all fluorescence, UV-Vis, and Circular Dichroism (CD) experiments. While MCP working concentrations are in the range of 0.5-5 μ M when titrating with BSA in fluorescence and CD experiments.

Fluorescence

The instrumental parameters for steady state fluorescence experiments were same as that of that reported earlier[6]. Briefly, excitation wavelength of 280nm is set for exciting intrinsic fluorophores of BSA and their corresponding emission spectra were recorded in the range of 300-500nm on Jasco J-815 spectropolarimeter. Further, the excitation and emission slit widths of 5nm and 10nm were set respectively with a detector voltage of 550V. Every measurement is accumulated twice with a scan

speed of 100nm/min having a data pitch of 1nm and the average of these two accumulations is taken for the final spectra. The final spectra are corrected for inner filter effect which is given by the following equation.

$$F_{\text{cor}} = F_{\text{obs}} \times e^{(A_{\text{exi}} + A_{\text{emi}})/2}$$

Wherein F_{cor} and F_{obs} are the corrected and observed fluorescence intensities respectively and A_{exi} and A_{emi} are the respective absorbance intensities at excitation and emission wavelengths of BSA protein. Site identification and temperature experiments were also performed under similar conditions as described above.

UV-Visible

The UV-Vis spectra of the interactions between MCP-BSA were monitored over a wavelength range of 220–350 nm using a double beam UV-Vis spectrophotometer (UV-1800SchimazuTM) (Schimazu Corporation, Tokyo, Japan).

Circular Dichroism

Secondary structural changes of BSA during interaction with MCP is studied by circular dichroism. CD experiments were performed on the same instrument where fluorescence experiments were carried out, (Jasco J-815 spectropolarimeter) using a quartz cell of length of 0.1cm in the Far UV range (190-300 nm) at room temperature by switching to CD mode. The scan speed of the instrument is set a 50nm/min with response time of 1s. BSA concentration is kept constant at a concentration of 0.5 μ M and titrated with increasing concentrations of MCP from 0.5-5 μ M. The observed CD is converted to mean residual ellipticity (MRE; deg cm² dmol⁻¹) by the following equation [7].

$$MRE = \frac{\text{observed CD (m deg)}}{C_p \times n \times l \times 10}$$

Where “Cp” denotes the molar concentration of BSA, “n” denotes the number of residues in the protein and “l” denotes the path length. This MRE

values at 208nm can be used to calculate the α -helical content of free BSA and MCP complexed BSA by the following equation[8,9].

$$\alpha - \text{helical (\%)} = \frac{-(MRE_{208} - 4000)}{33000 - 4000} \times 100$$

Where MRE_{208} are the measured MRE values and the constant values 33000 and 4000 denotes the MRE_{208} values of pure α -helix and β -form and random coil conformations respectively. Further analysis was done in GraphPad prism 8.0.

Molecular Docking

Autodock tools 4.2 of Scripps research institute is used for performing molecular modelling studies using Lamarckian genetic search algorithm for generating different conformations during course of interaction of MCP with BSA. To achieve this, crystal structure of BSA is obtained from protein data bank (PDB ID:4F5S) and the corresponding topology was prepared by autodock tools 4.2. PDB structure of MCP is obtained from zinc 15 database and is used without further modifications. Grid box of dimensions 126 x 85 x 100 was generated with grid spacing of 0.750 Å. And the center of the grid was set to 10.561, 21.667 and 101.207 nm. Docking parameters were set at its default settings and genetic algorithm search was used for generating the best 50 conformations. The conformer with lowest binding energy that corresponds to the experimental value is explored, visualized, and analyzed using PyMol and discovery studio software.

III. RESULTS AND DISCUSSIONS

Presence of intrinsic fluorophores, W134 and W213 in BSA structure alleviates the study of interactions of MCP with BSA by fluorescence technique. Fluorescence quenching studies provide beneficial information about the mechanism, strength, and the binding site of small molecules with the macromolecules. In some cases, it also provides the information regarding the active site of interaction of drugs. Mechanistically, fluorescence quenching is

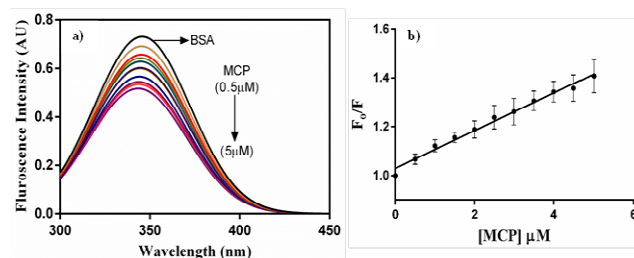
the consequence of interaction of small molecules with macromolecule via diversified mechanisms such as ground state complex formation, excited state reactions, molecular rearrangements, and energy transfer reactions to name a few. The exact nature of interactions can be arrived by successive treatment of quenching data by stern-volmer equations (discussed later). Hence in the present study we tried to understand the interaction mechanism of MCP with bovine serum albumin by fluorescence method. Tryptophan residues of BSA are in the hydrophobic cavities of domain IB and IIA however the hydrophobic peptide regions are present to a greater extent in domain IB[10]. Accessibility of these tryptophan residues to the polar environment due to the approach of drug molecules or solvent molecules decreases the fluorescence quantum yields [11]. On successive addition of 0.5 μ M concentrations of MCP up to a final concentration of 5 μ M of MCP the fluorescence intensity of BSA decreased in a concentration dependent manner (Figure 2). Further the emission maxima and peak shape of BSA remain unaltered throughout the course of addition of MCP indicating a weak interaction of MCP with BSA[12]. This result is of informative in that MCP might be approaching either of the tryptophan residues located at W134 or W213, since these are the intrinsic fluorophores that are mostly responsible for obtaining fluorescence in BSA molecule. Since W213 is present in proper hydrophobic binding pocket of subdomain IIA of BSA and most of the heterocyclic ligands are prone to bind to this binding pocket, we also presume that MCP, a structurally heterocyclic ligand, might also approach subdomain IIA of BSA[13-15]. Quenching of emission maxima due to the approach of MCP might occur either by forming a complex (Static quenching) or through collisions (Dynamic quenching). To further understand which mechanism of quenching is operative during interaction of MCP with BSA, the quenching data is treated with stern-volmer equation[16] as given below.

$$F_0/F = 1 + K_{SV}[Q] = 1 + K_q\tau_0[Q]$$

Where, F_0 and F are fluorescence intensities in the absence and presence of MCP, respectively. $[Q]$ denotes the quencher (MCP) concentration and K_{SV} is stern-volmer quenching constant. The stern-volmer quenching constant is the product of k_q (bimolecular quenching rate constant) and τ_0 (lifetime of the fluorophore in the absence of MCP, which is $\sim 10^{-8}$ s) and k_q can be obtained as given below

$$K_q = K_{sv}/\tau_0.$$

Fig. 2a) Fluorescence spectra of BSA (0.5 μ M) and BSA in the presence of increasing concentrations of MCP (0.5-5 μ M) and b) Stern-Volmer curve for binding of MCP with BSA



Treating the fluorescence quenching data with the above mentioned equation resulted in the quenching rate constant of $2.6 \pm 0.6 \times 10^{12} \text{ M}^{-1}\text{s}^{-1}$ which is found to be larger than the maximum diffusion collisional quenching rate constant for various quenchers in the presence of biopolymers (i.e $2.0 \times 10^{10} \text{ M}^{-1}\text{s}^{-1}$). This implies that static quenching might be operative during the interaction of MCP with BSA. Yet another way of affirming the type of quenching mechanism operative during the interaction of MCP with BSA is to study the behavior of stern-volmer plots at different temperatures. Therefore, stern-volmer plots at temperatures 288, 308 and 318 K were plotted and were found to be linear. Further it is noticed that at a given temperature the collisional quenching rate constant K_q are also found to be larger than the quenching rate constant of biopolymers suggesting a static quenching is operative at all studied temperatures. However, the K_q and K_{sv} values at respective temperatures are considerably high which are accounted for the increase in the quantum yield

of BSA and/or strong complexation of BSA with MCP at excited state[17,18]. At the studied temperatures the values of K_{SV} is found to be increasing with the increase in the temperature suggesting dynamic quenching is operative (Figure 3 and Table 1). From the outcomes of collisional rate constant and temperature studies it is undecipherable whether static and/or dynamic quenching is operative and which quenching mechanism is predominate.

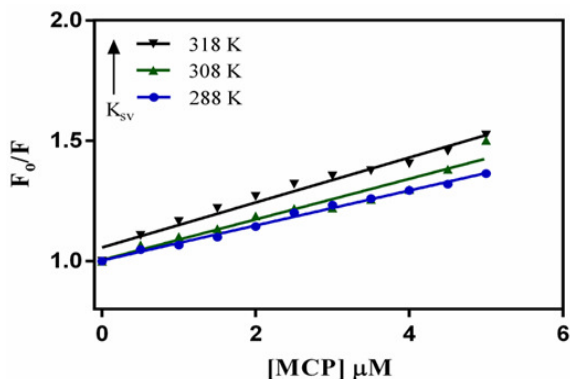


Fig. 3a) Stern-volmer Plots for MCP-BSA complex at 288, 308 and 318 K

TABLE I
STERN-VOLMER (K_{SV}), QUENCHING CONSTANT (K_q) OF MCP-BSA COMPLEX AT 288, 308 AND 318 K

T (K)	$K_{sv} \times 10^4 (M^{-1})$	$K_q \times 10^{12} (M^{-1} \cdot s^{-1})$
288	7.26	7.26
308	8.42	8.42
318	9.34	9.34

UV-Visible studies provide an alternative means of understanding the quenching mechanism though it does not give the information about the predominant quenching mechanism. Static quenching is the consequence of complex formation in the ground state however dynamic quenching results due to collisions in the excited state. Hence an increase in the absorption spectra of BSA in the presence of interacting partner indicates complex formation and further implies the operation of static quenching. Taking the advantage of this, the UV absorption

spectra of BSA with and without MCP was recorded and found that the absorption spectra of BSA at $\approx 280\text{nm}$ was increased when $5\mu\text{M}$ of MCP was added (Figure 4). However, MCP alone do not absorb at $\approx 280\text{nm}$ which is the characteristic absorption wavelength of BSA. Thus by, compiling the results of biomolecular quenching constants, temperature, and UV absorption studies it is understood that both static and dynamic quenching is operative during the interaction of MCP with BSA however static quenching is slightly dominating.

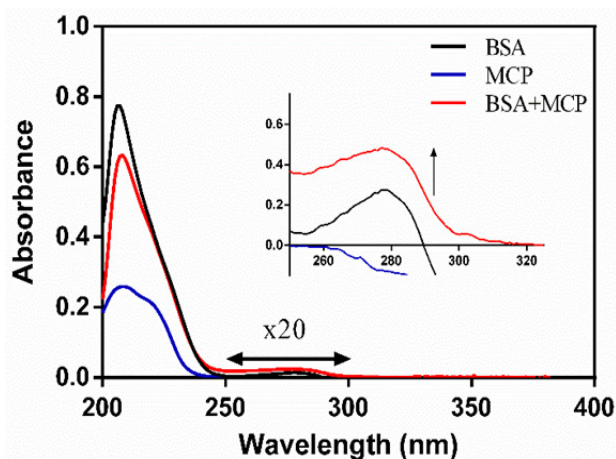


Fig. 4 UV absorption spectra of MCP, BSA and BSA-MCP complex at room temperature; [MCP]= $5\mu\text{M}$ and [BSA]= $1\mu\text{M}$

Most of the chemical entities become utilitarian drug molecules when they can bind macromolecules reversibly with moderate binding constants of $1-15 \times 10^4\text{M}^{-1}$ and thereby influencing the drug stability and toxicity during chemotherapeutic process. When the drug molecules bind solely to macromolecules of equivalent binding sites, then the concentration of free and bound molecules at equilibrium is given by the following equation[19].

$$\log (F_0-F)/F = \log K_b + n \log [Q]$$

Where K_b , n and $[Q]$ represents binding constant/association constant, number of binding sites and concentration of MCP respectively. Treatment of fluorescence quenching data obtained at the three different temperatures using the above equation resulted in the linear plots with binding

constants of $5.32 \pm 1.5 \times 10^4 \text{M}^{-1}$, $2.88 \pm 1.4 \times 10^4 \text{M}^{-1}$, $2.21 \pm 1.3 \times 10^4 \text{M}^{-1}$ at temperatures 288, 308 and 318 K respectively. From Figure 5a and Table 2, it is evident that the binding constant values are inversely related to the temperature, indicating the formation of considerable stable BSA-MCP complex [20,21]. Such an inverse relation suggests that there is a gradual decomposition of the complex with the raise in temperature thus leading to decrease in the binding constant values. Higher temperatures lead to faster diffusion thereby leading larger amounts of collisional quenching. The

Where K is the binding constant at the corresponding temperature T and R is the gas constant and the values of ΔH° and ΔS° were evaluated from the slope and intercept of the plots of $\ln K$ against $1/T$.

Complexes with positive enthalpy and entropy implies that the complexation is mainly entropy driven and enthalpy is unfavorable. Whereas the complexes with negative values of enthalpy and entropy implies that hydrogen bonding and vanderwaals plays a dominant role during

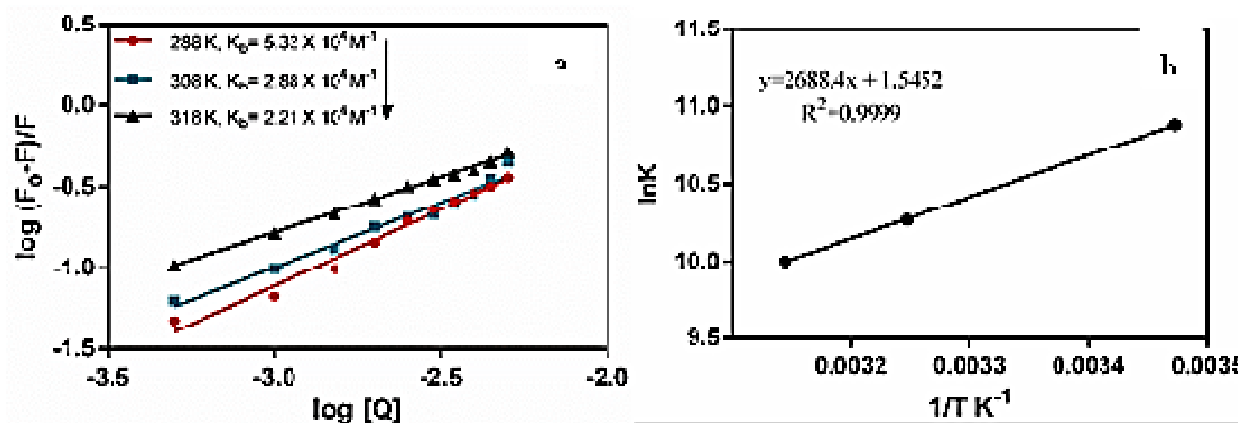


Fig. 5 a) $\log (F-F_0)/F$ Vs $\log [Q]$ plots for MCP-BSA complex at 288, 308, and 318 K. b) Van't Hoff plot for the binding of MCP with BSA

number of binding sites (n) is found to be 1 at all the studied temperatures thus indicating there exists one

binding site. The fundamental forces that are responsible for complex formation are hydrogen bonding, hydrophobic interactions, vanderwaals interactions and electrostatic interactions. However, these forces dominate one another in given complex. Further to elucidate the nature of forces that are responsible for the complexation of BSA-MCP, the thermodynamic parameters enthalpy (ΔH), entropy (ΔS) and free energy (ΔG) of the complex is calculated by using the Van't Hoff equation as given below.

$$\ln K = -\Delta H^\circ/RT + \Delta S^\circ/R$$

$$\Delta G^\circ = \Delta H^\circ - T\Delta S^\circ$$

complexation. Complexes having a positive entropy and negative enthalpy possess hydrophobic interactions and hydrogen bonding as the dominant forces. The negative value of enthalpy ($-22.35 \text{ kJ mol}^{-1}$) during BSA-MCP complex indicates that hydrogen bonding is formed exothermically ($\Delta H < 0$) [16]. This further illustrates that with increase in temperature the complex gradually decomposes leading to the decrease in the binding constant values at higher temperatures (Figure 5b and Table 2). The positive entropy during the BSA-MCP complex formation indicates that hydrophobic interactions also play role. Taken together, the BSA-MCP complex formation are stabilized by dominant hydrophobic interactions and hydrogen bond formation. The negative value of ΔG further reveals that the interaction process is spontaneous.

Hydrophobic pockets of macromolecules serve as the major depots for the small drug molecules for their interaction. Structural diversity of the drug molecules/ligands alters the domination of forces of interactions thus might even alter the site of interaction to have strong and stable complexation.

TABLE 2
BINDING CONSTANTS (K_b) OF MCP-BSA COMPLEX AT 288, 308
AND 318 K AND CORRESPONDING THERMODYNAMIC
PARAMETERS

T (K)	$K_b \times 10^4$ (M^{-1})	ΔH (kJ/mol)	ΔG (kJ/mol)	ΔS (J/mol K)
288	5.32	-22.35	-26.05	12.84
308	2.88		-26.31	
318	2.21		-26.44	

BSA being allosteric in nature it can accommodate more than one ligand in the same binding site simultaneously with minor or no conformational changes in the protein. This complicates the identification of exact location of binding site for the molecules/ligands. However, to date, literature findings [22,23] suggest that BSA possess two major drug binding sites located at subdomain IIA and IIIA which were also referred to as site I and site II respectively. In addition to these principal regions of drug binding, subdomain IB also serves as the secondary binding site for few molecules [24]. To explore the probable site of interaction of molecules with BSA, site specific probes i.e. phenylbutazone/warfarin and ibuprofen, were used in most of the studies [25,15]. Therefore, similar strategies were adopted in the present study to find the probable site of interaction of MCP with BSA. In such a strategy, it is presumed that the site markers (phenylbutazone or ibuprofen) will displace MCP from its binding site or alters the binding constant value of in the presence of site markers.

For site identification studies, $1\mu M$ of BSA sample were mixed with $5\mu M$ of MCP and incubated for 5min and thereafter it is titrated with site probes from a concentration of $0.5-5\mu M$. The corresponding fluorescence data were acquired by exciting the samples at 280nm. During titration with site probes there are no significant changes in the emission maxima and/or shape of the peak with gradual decrease in the fluorescence intensities (Figure 6a and 6b). This illustrates that minor

conformational changes occurred in BSA protein structure for accommodating the incoming site probes thus leading to disruption of the BSA-MCP complex. Further to understand in which case there is maximum disruption of the BSA-MCP complex, percentage of MCP displaced by the site markers was estimated by calculating the relative fluorescence (F_{Rel}) as given by Sudlow *et al* [26].

$$\% F_{Rel} = F/F_0 \times 100.$$

Where, F_0 and F are the corresponding fluorescence intensities of MCP-BSA complex in the absence and presence of site probes respectively. Further the obtained relative fluorescence data were plotted as against the concentrations of site probes under study (Figure 6c).

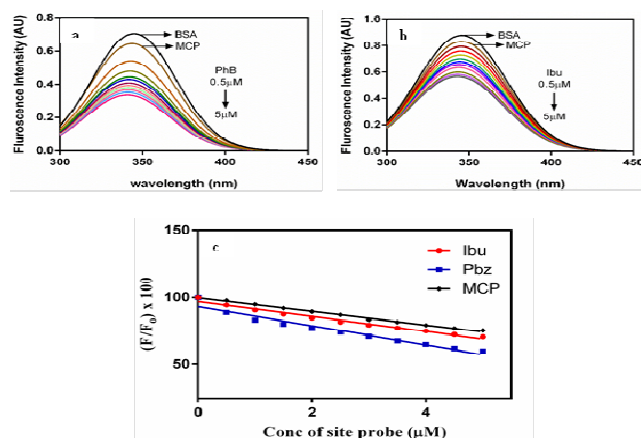


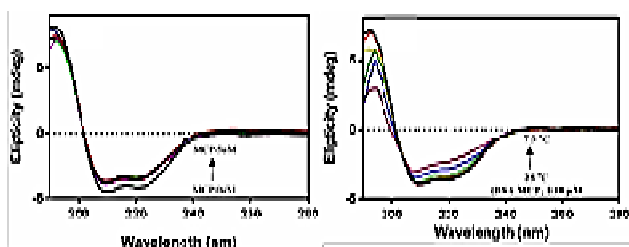
Fig. 6 Fluorescence quenching of MCP-BSA complex in the presence of site markers a) Phenylbutazone b) Ibuprofen c) Relative percentage quenching of fluorescence of MCP-BSA complex in the presence different concentrations of site markers

From Figure 6c it is evident that the percentage of decrease in the fluorescence intensity of the MCP-BSA complex is more in the presence of phenylbutazone site marker when compared to that of ibuprofen site marker. Such a decrease of fluorescence intensity implies that phenylbutazone disturbs MCP-BSA complex to a greater extent than that of ibuprofen. Hence it is inferred that the probable binding site of MCP is site I.

CD spectral studies provide insights into alterations of secondary structural elements during interactions

of small molecules with macromolecules. Therefore, to accomplish for the changes in the secondary structural elements that occur during the interaction of MCP with BSA, CD spectral analysis were taken up. The CD spectra of free BSA showed two characteristic negative bands at 208 nm and 222 nm which were originating due to $\pi \rightarrow \pi^*$ and $n \rightarrow \pi^*$ transitions of an α -helical peptide bond respectively. BSA in its unbound state exhibited 65% of α -helical content, however upon addition of $1 \mu\text{M}$ MCP the α -helical content was reduced to 57% and this was reached to 59% upon sequential addition of $1 \mu\text{M}$ MCP to a final concentration of $5 \mu\text{M}$ MCP (Figure 7). Further, the shapes of these two negative bands were found to be similar both in presence and absence of MCP. Such a decrease in α -helical content without alternations in the band shapes would infer that MCP might brought slight conformational changes in the BSA protein to form a complex by disturbing the hydrogen bonding networks of the amino acid residues of main polypeptide chain of BSA [27,28]. This further indicates that the complexation of MCP with BSA with minor conformational changes has occurred.

Fig. 7 CD spectra of a) BSA ($0.5 \mu\text{M}$) with varying concentrations of MCP (0 - $5 \mu\text{M}$) b) Thermal stability of MCP-BSA complex with increase in temperature (25 - $75 \text{ }^\circ\text{C}$)



In addition to this conformational analysis we also attempted to study the effect of temperature on the stability of the MCP-BSA complex by CD studies. To execute these experiments, the complex formed at 1:10 ratio of BSA:MCP is subjected to different temperatures ranging from 25 - $75 \text{ }^\circ\text{C}$ with a temperature interval of $10 \text{ }^\circ\text{C}$. At $25 \text{ }^\circ\text{C}$, the complex under study exhibited 59% of α -helical content which was slightly decreased when the temperature was reached to $55 \text{ }^\circ\text{C}$. Further increase in temperature caused a loss of $\approx 5\%$ of α -helical

content which was further lost to $\approx 4\%$ at temperatures $65 \text{ }^\circ\text{C}$ and $75 \text{ }^\circ\text{C}$ respectively. Outcome of these studies implies that the formed complex is stable up to $55 \text{ }^\circ\text{C}$ and the complex starts dissociating at $65 \text{ }^\circ\text{C}$. This further corroborates the decrease in the binding constant values with the increase of temperature as obtained from fluorescence studies.

Though solution phase experiments allow the identification of interaction mechanisms of drug molecules with the biomolecules at physiological conditions they lack to provide atomistic view of interactions.

Molecular modeling methods subdue these limitations to understand the interactions at atomistic level besides corroborating experimental outcomes [28,29]. Therefore, to further understand the nature of interactions that drive the MCP-BSA complex formation molecular docking studies were performed. To find the best binding pocket for MCP 50 conformations were generated. Among the generated conformations, the conformation with the best fit and lowest binding energy is found at the adjunction of domain I and II with a free energy change of $-6.39 \text{ Kcal mol}^{-1}$ (Figure 8) thus complimenting fluorescence data. Upon further investigation of the complex, it was found that MCP is stabilized by three hydrogen bonds which are formed between the free amine hydrogens of MCP and TRY84 and ASP86 at 3.49 , 4.12 and 6.13 \AA . Furthermore, MCP is stabilized by van der Waals interactions by the residues of the domain I as shown in Figure 8. In addition to these interactions the phenyl group of MCP also involved in the hydrophobic interactions with the phenyl ring of TRY84 at 4.89 \AA and Sulphur atom of MET87 at 5.72 \AA respectively.

Taking BSA as a model protein, we explored the possible means of bioavailability and advantages of MCP over other antidepressants that were in current use for treating depression. Fluorescence studies relieved that MCP interacts with BSA with a moderate binding constant of $5.32 \pm 1.5 \times 10^4 \text{ M}^{-1}$. Fluorescence and UV-Vis studies emphasize that the

interactions involved are mainly due complex formation besides collisions. Thermodynamic parameters indicate that MCP-BSA complex formation is spontaneous wherein hydrogen bonding and hydrophobic interactions play dominant role for stabilizing the complex. Further analysis of MCP-BSA complex by CD spectroscopy suggested that the secondary structural elements of the native BSA was slightly affected upon complexation with MCP. However, the complex is stable up to 55°C. The percentage relative fluorescence quenching studies with site markers indicates that MCP interacts with BSA residues near to site I. This is further corroborated by molecular docking studies which showed that TRY84 and ASP86 are involved in hydrogen bonding whereas TRY84 and MET87 are involved in hydrophobic interactions. Thus, moderate binding of MCP to the model transporting protein with minor secondary structural changes can be attributed for the high bioavailability of MCP. This makes it a choice of drug to prescribe for treating depression.

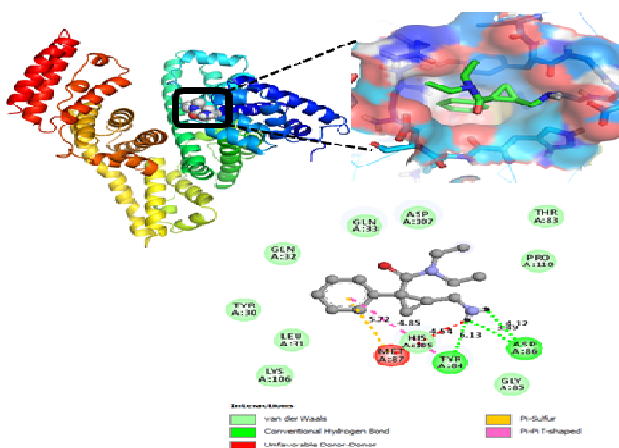


Fig. 8 Schematic view of the docked conformer of MCP-BSA complex with lowest binding energy and zoomed view showing hydrogen bonding distances along with interacting amino acids

IV. CONCLUSION

MilancipranHCl (MCP), an antidepressant drug used for treating depression belongs to serotonin and norepinephrine reuptake inhibitor class of

compounds. High bioavailability of MCP besides its rapid absorption and elimination makes it a selective drug for prescription. On the other hand, MCP has poor affinity towards transporting proteins. To date, there are no detailed studies which accounts for the poor affinity of MCP with transporting proteins. Herein the present study brings out the binding capacity of MCP with model transporting protein BSA by spectroscopic and molecular modelling studies. Fluorescence studies demonstrated that MCP interacts with BSA with a binding constant of $5.32 \pm 1.5 \times 10^4 \text{M}^{-1}$ by forming complex (static quenching) besides collisions (dynamic quenching). During interaction with MCP, 6% of helical content of BSA was reduced and formed complex is stable up to 75°C as evident from CD studies. MCP interacts with BSA at junction of domain I and domain II by forming hydrogen bonds with TYR 89 and ASP 86 and the aromatic ring of MCP involves in the hydrophobic interactions (Pi-Pi and Pi-Sulphur).

Conflicts of interest:

Declared None.

Acknowledgments:

None

REFERENCES:

1. Tennouga L, Haouaria M. Kinetic Study of the Controlled Release of Procaine Grafted in Monomer and Copolymer Supports in both Homogeneous and Heterogeneous Medium. *Am J PolymSci* 2013;99-106.
2. Stamler J, Singel D, Loscalzo J. Biochemistry of Nitric Oxide and Its Redox-Activated Forms. *Science* 1992;258(5090):1898-1902.
3. He XM, Carter DC. Atomic Structure and Chemistry of Human Serum Albumin. *Nature* 1992;358(6383):209-215.
4. Ashoka S, Seetharamappa J, Kandagal PB, Shaikh SMT. Investigation of the Interaction between Trazodone Hydrochloride and Bovine Serum Albumin. *J Lumin* 2006;121(1):179-186.
5. Peters T. Serum Albumin. In: Anfinsen CB, Edsall JT, Richards FM, editors. *Adv. Protein Chem.* 37: Academic Press; 1985. p. 161-245.
6. Somaji L, Rapolu R. Binding Studies of Valganciclovir to Human Serum Albumin by Multispectroscopic Techniques. *Int J Pharm PharmSci* 2018;10(10):87-92.
7. Chen Y-H, Yang JT, Martinez HM. Determination of the Secondary Structures of Proteins by Circular Dichroism and Optical Rotatory Dispersion. *Biochemistry* 1972;11(22):4120-4131.
8. Gao H, Lei L, Liu J, Kong Q, Chen X, Hu Z. The Study on the Interaction between Human Serum Albumin and a New Reagent with Antitumor Activity by Spectroscopic Methods. *J PhotochemPhotobiol A Chem* 2004;167:213-221.
9. Giménez RE, Vargová V, Rey V, Turbay MB, Abatedaga I, MoránVieyraFE et al. Interaction of Singlet Oxygen with Bovine Serum

- Albumin and the Role of the Protein Nano-Compartmentalization. *Free RadicBiol Med* 2016;94:99-109.
10. Jeremias HF, Lousa D, Hollmann A, Coelho AC, Baltazar CS, SeixasJDet al. Study of the Interactions of Bovine Serum Albumin with a Molybdenum(II) Carbonyl Complex by Spectroscopic and Molecular Simulation Methods. *PLoS One* 2018;13(9):e0204624.
 11. Bi S, Song D, Tian Y, Zhou X, Liu Z, Zhang H. Molecular Spectroscopic Study on the Interaction of Tetracyclines with Serum Albumins. *SpectrochimActa A MolBiomolSpectrosc* 2005;61(4):629-636.
 12. Sudlow G, Birkett DJ, Wade DN. Further Characterization of Specific Drug Binding Sites on Human Serum Albumin. *MolPharmacol* 1976;12(6):1052-1061.
 13. Varshney A, Sen P, Ahmad E, Rehan M, Subbarao N, Khan RH. Ligand Binding Strategies of Human Serum Albumin: How Can the Cargo Be Utilized? *Chirality* 2010;22(1):77-87.
 14. Curry S. Lessons from the Crystallographic Analysis of Small Molecule Binding to Human Serum Albumin. *Drug MetabPharmacokinet* 2009;24(4):342-357.
 15. He Y, Wang Y, Tang L, Liu H, Chen W, ZhengZet al. Binding of Puerarin to Human Serum Albumin: A Spectroscopic Analysis and Molecular Docking. *J Fluoresc* 2008;18(2):433-442.
 16. Ross PD, Subramanian S. Thermodynamics of Protein Association Reactions: Forces Contributing to Stability. *Biochemistry* 1981;20(11):3096-3102.
 17. Han X-L, Mei P, Liu Y, Xiao Q, Jiang F-L, Li R. Binding Interaction of Quinlorac with Bovine Serum Albumin: A Biophysical Study. *SpectrochimActa A MolBiomolSpectrosc* 2009;74(3):781-787.
 18. Xu H, Liu Q, Wen Y. Spectroscopic Studies on the Interaction between Nicotinamide and Bovine Serum Albumin. *SpectrochimActa A MolBiomolSpectrosc* 2008;71(3):984-988.
 19. Hu Y-J, Liu Y, Shen X-S, Fang X-Y, Qu S-S. Studies on the Interaction between 1-Hexylcarbonyl-5-Fluorouracil and Bovine Serum Albumin. *J MolStruct* 2005;738:143.
 20. Sudlow G, Birkett DJ, Wade DN. The Characterization of Two Specific Drug Binding Sites on Human Serum Albumin. *MolPharmacol* 1975;11(6):824-832.
 21. Kandagal PB, Shaikh SMT, Manjunatha DH, Seetharamappa J, Nagaralli BS. Spectroscopic Studies on the Binding of Bioactive Phenothiazine Compounds to Human Serum Albumin. *J PhotochemPhotobiol A Chem* 2007;189(1):121-127.
 22. Yamasaki K, Chuang V, Maruyama T, Otagiri M. Albumin-Drug Interaction and Its Clinical Implication. *BiochimBiophysActa* 2013;1830:5435-5443.
 23. Nagati V, Kallubai M, Chinthapalli DK, Subramanyam R. Exploration of Binding Studies of B-Oxalyldiamino Propionic Acid (β -ODAP), a Non-Protein Amino Acid with Human Serum Albumin-Biophysical and Computational Approach. *J BiomolStructDyn* 2019;37(15):3914-3922.
 24. Nerusu A, Chinthapalli DK, Subramanyam R. Role of Herborn (K240E) and Milano Slow (D375H) Human Serum Albumin Variants Towards Binding of Phenylbutazone and Ibuprofen. *Int J BiolMacromol* 2019;134:645-652.
 25. Guo X-j, Jing K, Guo C, Jiang Y-c, Tong J, Han X-w. The Investigation of the Interaction between Oxybutynin Hydrochloride and Bovine Serum Albumin by Spectroscopic Methods. *J Lumin* 2010;130(12):2281-2287.
 26. Hu Y-J, Liu Y, Wang J-B, Xiao X-H, Qu S-S. Study of the Interaction between MonoammoniumGlycyrrhizinate and Bovine Serum Albumin. *J Pharma Biomed Anal* 2004;36(4):915-919.
 27. Xu H, Yao N, Xu H, Wang T, Li G, Li Z. Characterization of the Interaction between Eupatorin and Bovine Serum Albumin by Spectroscopic and Molecular Modeling Methods. *Int J MolSci* 2013;14(7):14185-14203.
 28. Morris GM, Huey R, Lindstrom W, Sanner MF, Belew RK, GoodsellSet al. Autodock4 and Autodocktools4: Automated Docking with Selective Receptor Flexibility. *J ComputChem* 2009;30(16):2785-2791.
 29. Shi JH, Pan DQ, Wang XX, Liu TT, Jiang M, Wang Q. Characterizing the Binding Interaction between Antimalarial Artemether (Amt) and Bovine Serum Albumin (BSA): Spectroscopic and Molecular Docking Methods. *J PhotochemPhotobiol B* 2016;162:14-23.